Journal of The Electrochemical Society, **150** (4) C208-C211 (2003)
0013-4651/2003/150(4)/C208/4/$7.00 © The Electrochemical Society, Inc.

Etch Pit Observation for 6H-SiC by Electrochemical Etching Using an Aqueous KOH Solution

Masashi Kato,[a,z] Masaya Ichimura,[a,*] Eisuke Arai,[a] and Perumalsamy Ramasamy[b]

[a]*Department of Electrical and Computer Engineering, Nagoya Institute of Technology, Showa, Nagoya 466-8555, Japan*
[b]*Crystal Growth Center, Anna University, Chennai 600-25, India*

n-Type 6H-SiC bulk crystals were etched by an electrochemical method using an aqueous KOH solution as an electrolyte. After etching using a 50 wt % KOH solution at room temperature, etched samples showed etch pits which are always pairs of a crescent (or a circle) shaped pit and a triangle-shaped pit. The paired pits align in the radial direction from the wafer center and the triangle pit is in the wafer perimeter side with its base facing the perimeter. From comparison with optical microscope observation and also with molten KOH etching, it was found that the origin of the electrochemically formed etch pits is not only micropipe but also some other kind of defects, which is most probably screw dislocation.
 [DOI: 10.1149/1.1554918]

Manuscript submitted June 3, 2002; revised manuscript received October 2, 2002. Available electronically February 25, 2003.

SiC has wide bandgap, high thermal conductivity, high electron saturation velocity, and high physicochemical stability. These properties make SiC promising for high-power electronic devices operating in high temperature and high radiation environment.[1] Recently, SiC crystalline quality has become much better than in past decades, and successful fabrication of electronic devices using SiC has been reported by many research groups. However, SiC crystal has many structural defects which deteriorate performance of the devices. The most well-known structural defect observed in SiC is micropipes, which is a hollow core threading through the entire SiC wafer. Other structural defects in SiC are dislocations, voids, inclusions, etc. All kinds of structural defects should be eliminated for electronic device fabrication and usage as substrates for epitaxial growth of GaN and SiC. In order to eliminate these defects, defect characterization is important.

Usually, structural defects in SiC crystals are revealed by molten KOH etching.[2-11] This etching proceeds preferentially at a structural defect position and thus defects such as micropipes and dislocations appear as etch pits.[2,11] In this study, we employed another etching method for characterization of the defects, *i.e.*, an electrochemical etching method. In this method, we apply anodic voltage to the SiC sample in an aqueous KOH solution electrolyte, and then etching occurs at a region of the sample exposed to the electrolyte. The electrochemical etching of SiC using an aqueous KOH solution has been reported in Ref. 12. The etching mechanism of the electrochemical method differs from the molten KOH etching, and the resulting etched surfaces are also different between them. In this paper, we observed etch pit morphology of the electrochemically etched SiC sample surfaces and compared it with an etch pit morphology of a molten KOH etched surface.

Experimental

The electrochemical etching was performed for commercially available n-type 6H-SiC (0001) wafers with both sides polished. The net donor concentration of the wafers is approximately 10^{18} cm^{-3}. The wafers were cut into small pieces with dimension of 5 mm × 1 cm. Before the etching, ohmic Al contacts were evaporated on the Si face of the samples. Each sample was placed on a plastic plate, and its edge part, the contacts, and the lead wire were covered with silicone resin. The contents of KOH in the aqueous solution for an electrolyte was 50 wt %. The SiC samples and a Pt electrode were dipped in the electrolyte as an anode and a cathode, respectively. The voltage was applied between them at a constant current mode. The etching temperature was room temperature. Current density at the sample surface was fixed at 5 mA/cm^2 and etching time was 30 min. After the etching, the silicone resin was removed by a mixed solution of HF and HNO_3. The etching was done for both the Si face and the C face of the samples under the same condition. Etched surfaces were observed by a Nomarski microscope, a scanning electron microscope (SEM), and an atomic force microscope (AFM). In order to clarify the micropipe positions in the as-received sample, an optical microscope with crossed polarizer, which can reveal stress fields introduced by micropipes,[13] was employed. After the electrochemical etching, one sample was etched by molten KOH etching at 490°C for 10 min.

Results

As-received sample surfaces show no obvious structural defects or polishing scratches even in observation by the Nomarski microscope. During the electrochemical etching, applied voltage was around 25 V under the constant current condition described for all the samples. On the electrochemical etched surfaces, scratches and many etch pits with a peculiar shape are found as shown in Fig. 1a. This figure is for the Si face of the sample. Since the results in this study were almost the same for the Si and C faces, in this paper we show data only for the Si face. In this etching condition, the etched depth measured by the profilometer is approximately 30 nm, which is almost unchanged with increasing etching time because the etching proceeds with porous formation as described later. A white colored region at the left side in Fig. 1a was covered by silicone resin during the etching. After the etching, the scratches are clearly observed as seen in Fig. 1a. This implies that the sample has damages originating from polishing even though no scratches are observed before the etching. Figure 1b is a magnified picture of the etch pit. From Fig. 1a, each of the etch pits seems to consist of a crescent pit (or sometimes circle pit) and a triangle pit, and all the etch pits have almost the same size; the diameter of the crescent pit and the side of the triangle pit are about 10 μm. There is a dark point in the region surrounded by the crescent pit as shown in Fig. 1b, and it is a small circular pit. In the etch pits in Fig. 1a, some of the etch pits have the dark point and the others seem not to have the dark point. The crescent pit and the triangle pit align in the same direction for all the etch pits in Fig. 1a. It has been reported that only round-shaped etch pits are formed by an electrochemical etching,[12,14] and to the best of our knowledge, etch pits of this kind have never been reported in molten KOH etching.[2-11]

We performed the electrochemical etching in the same condition for SiC wafers supplied from four different venders. We observed this kind of etch pit for the wafers from two of the four venders. Thus, although that peculiar etch pit is not specific to one vender, the etch pit appearance may depend on crystal growth conditions. The results were reproducible for different wafers from the same vender.

* Electrochemical Society Active Member.
z E-mail: mkato@hermite.elcom.nitech.ac.jp

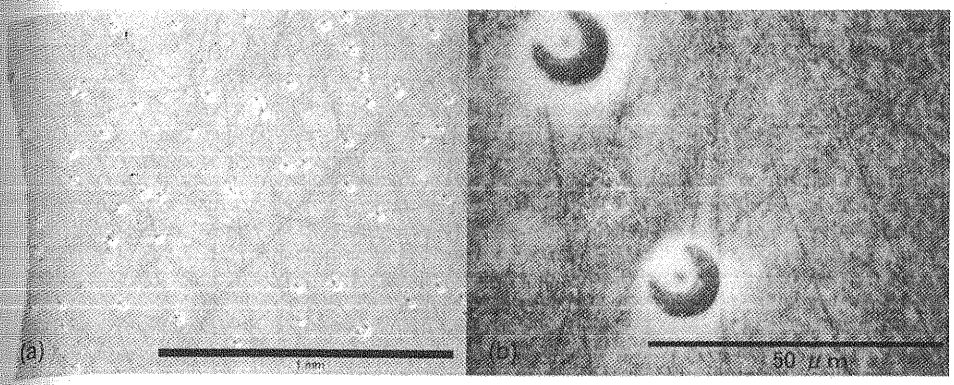

Figure 1. Optical micrographs for electrochemically etched 6H-SiC: (a) overview of etched surface and (b) magnified view at the etch pit point.

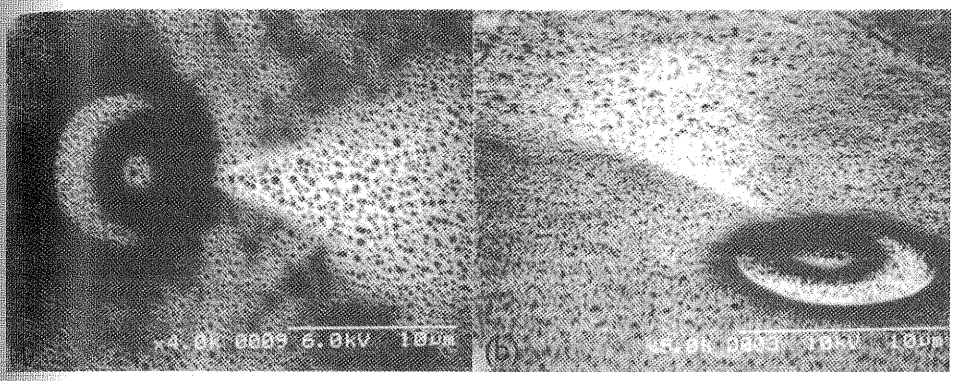

Figure 2. SEM micrograph for the etch pit: (a) perpendicular view from the surface and (b) inclined view of the same etch pit.

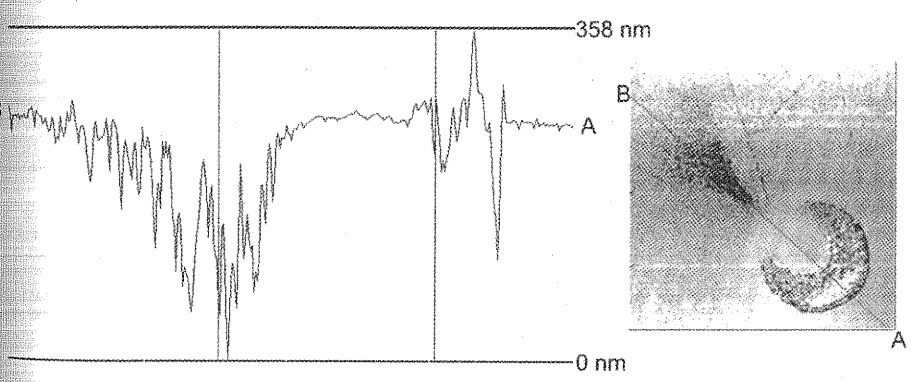

Figure 3. Cross-sectional profile for the etch pit taken by AFM.

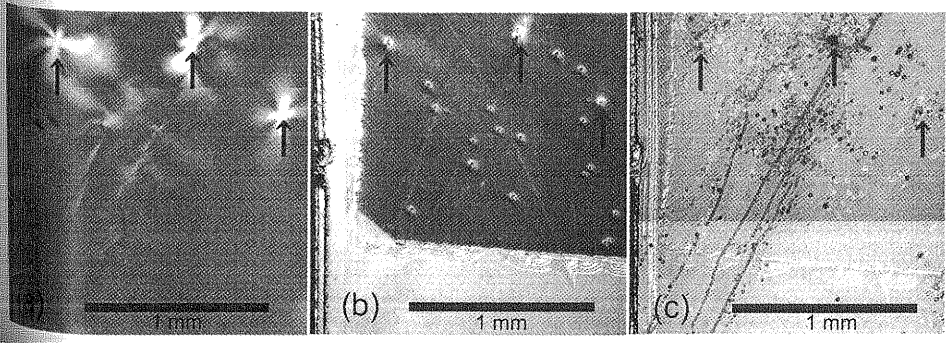

Figure 4. Optical micrograph for 6H-SiC: (a) as-received surface observed with crossed polarizer, (b) electrochemically etched surface for the same region, and (c) molten KOH etched surface for the same region. The arrows indicate the position of micropipes.

Figure 2a and b shows SEM micrographs for the etch pit. Figure 2a is a picture of perpendicular view and Fig. 2b is an inclined view. Almost all the surface areas become porous except for the region around the crescent pit. It seems that the dark point surrounded by the crescent pit observed in Fig. 1b has porous structure. The boundary of the triangle pit is unclear, especially in Fig. 2b. In order to see rise and fall around the etch pits in detail, we took an AFM image around an etch pit with a cross-sectional profile which is shown in Fig. 3. The cross-sectional line AB (the left side of the figure) corresponds to the line AB in the AFM image (the right side of the figure). From this figure, the crescent pit is mostly depressed, but there is an uplifted region in the middle part of the crescent pit. In Fig. 2b no such uplifted region is observed in the crescent pit. Therefore, the crescent pits are usually just depressed but some of them have uplifted regions. The triangle pit is depressed by 250 nm at its vertex near the crescent pit.

We also performed etchings under other conditions, *i.e.*, at lower KOH concentrations and higher or lower temperature ranges. The crescent or circle pits appeared under the other etching conditions but the triangle pits did not appear. In addition, the etching under the condition described previously reveals crescent or circle pits most clearly and makes the etched surfaces most porous. Thus, we think that the etch pit shape is related to the porosity.

The etch pit density ($\sim 10^3$ cm^{-2}) is one order of magnitude larger than the micropipe density nominally announced by the wafer vender (~ 100 cm^{-2}). In order to clarify correlation between the etch pits and micropipes, we observed optical micrographs with crossed polarizer for the as-received sample and for the same sample after the electrochemical etching. Figures 4a and b show the optical micrographs with crossed polarizer for the as-received surface and for the etched surface, respectively. Both images are for the same position within the sample. In Fig. 4a, three bright spots are observed. The center of these spots corresponds to the micropipe positions.[13] In Fig. 4b, the dark area is the etched part, and many white points corresponding to the etch pits appear there. By comparing the micropipe positions with the etch pit positions in these figures, we can see that all the micropipes become the etch pits after the electrochemical etching. Thus, all the micropipes become the etch pits. However, the number of the etch pits is obviously larger than that of the micropipes. Therefore the etch pits originate not only from micropipes but also from other kinds of defects.

Figure 4c shows the molten KOH etched surface for the same area of the sample. Etch pit density revealed by the molten KOH etching is almost the same as the nominal etch pit density announced from the wafer vender ($\sim 10^4$ cm^{-2}) and is larger by one order of magnitude than those revealed by the electrochemical etching. From these figures, we cannot clearly see that the defects revealed by the electrochemical etching become the etch pits in the molten KOH etching, because the etch pit density after the molten KOH etching is too high to confirm one-to-one correspondence.

Discussion

The direction of the paired etch pits formed by the electrochemical etching is almost the same within one sample as shown in Fig. 1a. However, from the observation of many pieces cut from one wafer, we found that the paired etch pits align in the radial direction from the wafer center irrespective of Si face or C face, as illustrated in Fig. 5b. The arrows in Fig. 5b indicate the direction of the etch pits, which is defined in Fig. 5a. From this fact, we can make a hypothesis about the cause of this peculiar-shaped etch pit. If the SiC crystal grows at steps of the spiral originating from a screw dislocation at the center of the wafer according to the Burton-Cabrera-Frank (BCF) theory,[15] the growth proceeds from the center of the wafer to its perimeter it with migrating steps. When there are obstacles, for example, micropipes or inclusions, on the growing surface, the migration of steps is stopped there. A schematic diagram of this situation is drawn in Fig. 6. As a result, in a region near the obstacles in the lower terrace, the crystal does not grow in the step-flow mode. In that region, which would have almost triangle shape,

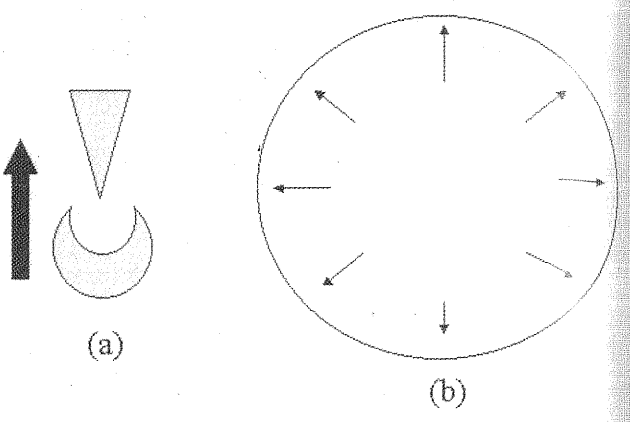

Figure 5. Schematic diagram of the direction of the etch pits.

crystalline quality would differ from the normal step-flow growth region. The electrochemical etching would disclose the crystalline quality difference originating from the growth mode difference. The pinning of steps by screw dislocations was observed for 6H-SiC.[10,16] From our data and these reports, it is most probable that the screw dislocations as well as micropipes cause the electrochemical etch pits. The screw dislocations form a vertical step on the step-flowing terrace, which can be the obstacles for the step-flow growth, but threading edge dislocations do not form such steps since their Burgers vectors are parallel to the surface. Sanchez *et al.* have reported that the screw dislocation density is one or two orders of magnitude lower than the edge dislocation density.[16] As noted previously, the electrochemical etch pit density is one order of magnitude lower than the molten KOH etch pit density. This density difference can be consistently explained considering that although both the edge and screw dislocations are revealed by the molten KOH etching, only the screw dislocations become etch pits in the electrochemical etching.

Although we tried to clarify the difference between the pit region and the rest by microscope Raman scattering, we did not find any Raman peak shifts for both TO and LO modes, whose wave numbers depend on stress and carrier concentration in the crystal, respectively.[17] Therefore we cannot confirm that stress and carrier concentration differences in the crystal are the cause of the triangle-shaped pits.

In the electrochemical etching, reaction species at the semiconductor-electrolyte interfaces are usually positive holes and negative-charged hydroxyl ions.[18-21] Thus, etching reaction requires holes at the semiconductor surfaces. In this study, since we did not use any light sources to generate electron-hole pairs in the sample

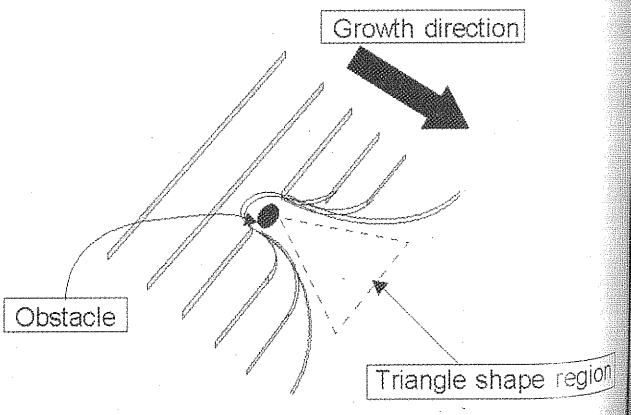

Figure 6. Schematic diagram for the creation mechanism of a triangle shape with different crystallinity from the other region during crystal growth.

surfaces, holes were produced by another process in the samples. Since SiC has a wide bandgap, thermal generation of electron-hole pairs hardly occurs at room temperature. Another possible hole creation mechanism is an impact ionization process. As noted earlier, this etching was performed at applied voltage of about 25 V. For 6H-SiC with donor concentration of 10^{18} cm^{-3}, this voltage makes an electric field high enough (3×10^6 V/cm) to cause the impact ionization at the sample surfaces, if the sample-electrolyte interface has an ideal Schottky barrier.[22,23] In fact, at a lower anodic voltage of 10 V, for example, no etching phenomenon was observed. Thus, we think that the etching proceeds with hole creation by the impact ionization process. The appearance of the etch pits implies that the impact ionization coefficient at the etch pit points is different from that in the rest of the surface. If the etch pits originate from the enhanced impact ionization coefficient, it is natural that they can be observed after the electrochemical etching but not after the molten KOH etching. It is unclear what kind of defects give rise to the enhancement of the impact ionization. Considering the results of the microscope Raman measurements, the enhancement would be due to some subtle difference in crystallinity or impurity concentration. Even in the electrochemical etching, when the KOH concentration or temperature was changed, the etch pits did not appear. Since the impact ionization coefficient depends on temperature and the electric field, its difference seems clear only in the etching under the conditions employed in this paper.

Kayambaki *et al.* have reported that electrochemical etching with an aqueous KOH solution results in quite different morphologies between the Si and C faces for 4H- and 6H-SiC.[12] However, we did not find significant difference between the Si and C faces in the present etching condition. Kayambaki *et al.* have also reported that round-shaped etch pits appear after the electrochemical etching.[12] Their results and our results are quite different. Their data for Si face etching are for epitaxial layer etching, but our samples are bulk 6H-SiC. They employed p-type SiC while our sample is n-type SiC. Since p-type SiC has many positive holes in thermal equilibrium, the impact ionization process is unnecessary for the reaction with hydroxyl ions. They employed a 0.05 M KOH electrolytic solution, which is two orders of magnitude lower concentration than that employed in this study. We may expect that these differences cause the large difference in the experimental results.

As shown in Fig. 1a, the electrochemical etching revealed the scratches originating from polishing. Thus, this etching method can detect the polishing damage even though the damage is invisible before etching. We observed the scratches for the wafers from the four venders, and the concentration of the scratches was different among venders.

Conclusions

n-type 6H-SiC samples were electrochemically etched using an aqueous KOH solution as an electrolyte. Etched surfaces showed many triangle-shaped etch pits accompanied by a crescent or a circle etch pit. The paired pits aligned in the radial direction from the wafer center. The triangle pit was in the wafer perimeter side with its base facing the perimeter. From optical microscope observation with crossed polarizer, the origin of the etch pit was not only micropipe but also other kinds of defects, most probably screw dislocations.

Acknowledgments

The authors are grateful to Professor H. Ohsato of Nagoya Institute of Technology and A. Okamoto of Toyota Central Research and Development Laboratory for their fruitful comments, and Professor S. Nishino, Dr. M. Sasaki, and T. Nishiguchi of Kyoto Institute of Technology for technical help in the molten KOH etching.

Nagoya Institute of Technology assisted in meeting the publication costs of this article.

References

1. G. L. Harris, *Properties of Silicon Carbide*, INSPEC, IEE, London (1995).
2. S. Ha, N. T. Nuhfer, G. S. Rohrer, M. D. Graef, and M. Skowronski, *J. Cryst. Growth,* **220**, 308 (2000).
3. M. Tuominen, R. Yakimova, R. C. Glass, T. Tuomi, and E. Janzén, *J. Cryst. Growth,* **144**, 267 (1994).
4. J. Takahashi, M. Kanaya, and Y. Fujiwara, *J. Cryst. Growth,* **135**, 61 (1994).
5. E. K. Sanchez, J. Q. Liu, M. De Graef, M. Skowronski, V. M. Vetter, and M. Dudley, *J. Appl. Phys.,* **91**, 1143 (2002).
6. M. Masakazu, N. Ohtani, T. Aigo, T. Fujimoto, H. Tsuge, H. Yashiro, and M. Kanaya, *J. Cryst. Growth,* **216**, 256 (2000).
7. M. Tuominen, R. Yakimova, A. Vehanen, and E. Janzén, *Mater. Sci. Eng., B,* **B57**, 228 (1999).
8. J. Takahashi, N. Ohtani, and M. Kanaya, *J. Cryst. Growth,* **167**, 596 (1996).
9. J. Takahashi, N. Ohtani, M. Katsuno, and S. Shinoyama, *J. Cryst. Growth,* **181**, 229 (1997).
10. N. Sugiyama, A. Okamoto, K. Okumura, T. Tani, and N. Kamiya, *J. Cryst. Growth,* **191**, 84 (1998).
11. M. Syväjärvi, R. Yakimova, and E. Janzén, *J. Electrochem. Soc.,* **147**, 3519 (2000).
12. M. Kayambaki, K. Tsagaraki, V. Cimalla, K. Zekentes, and R. Yakimova, *J. Electrochem. Soc.,* **147**, 2744 (2000).
13. T. Kato, H. Ohsato, A. Okamoto, N. Sugiyama, and T. Okuda, *Mater. Sci. Eng., B,* **56**, 263 (1998).
14. M. Kayambaki and K. Zekentes, *Mater. Sci. Forum,* **338-342**, 1061 (2000).
15. W. K. Burton, N. Cabrera, and F. C. Frank, *Philos. Trans. R. Soc. London, Ser. A,* **A243**, 299 (1951).
16. E. K. Sanchez, S. Ha, J. Grim, M. Skowronski, W. M. Vetter, M. Dudley, R. Bertke, and W. C. Mitchel, *J. Electrochem. Soc.,* **149**, G131 (2002).
17. S. Nakashima and H. Harima, *Phys. Status Solidi A,* **162**, 39 (1997).
18. J. E. Spanier, A. C. West, and I. P. Herman, *J. Electrochem. Soc.,* **148**, C663 (2001).
19. I. Lauermann, R. Memming, and D. Meissner, *J. Electrochem. Soc.,* **144**, 73 (1997).
20. M. Gleria and R. Memming, *J. Electroanal. Chem.,* **65**, 163 (1975).
21. J. S. Shor and A. D. Kurtz, *J. Electrochem. Soc.,* **141**, 778 (1994).
22. M. Ruff, H. Mitlehner, and R. Helbig, *IEEE Trans. Electron Devices,* **41**, 1040 (1994).
23. R. Raghunathan and B. J. Baliga, *Solid-State Electron.,* **43**, 199 (1999).